Momentum Transport in TCV Across Sawteeth Events

B. P. Duval 1), A. Bortolon 2), L. Federspiel 1), F. Felici 1), I. Furno 1), A. Karpushov 1), J. Paley 1), F. Piras 1) and the TCV team*

1) École Polytechnique Fédérale de Lausanne (EPFL), Centre de Recherches en Physique des Plasmas (CRPP), Association EURATOM-Confédération Suisse, 1015 Lausanne, Switzerland
2) Princeton Plasma Physics Laboratory, Princeton University, New Jersey 08543, USA

E-mail contact of main author: basil.duval@epfl.ch

Abstract. The Charge Exchange Recombination diagnostic on the TCV tokamak has been configured to measure the evolution of the Toroidal plasma rotation across sawteeth events. Previous measurements showed a strong discontinuity in the Toroidal rotation profile at the sawtooth inversion radius (the $q = 1$ radius) for a wide range of safety factors that limited the maximum intrinsic rotation values (i.e. the plasma rotation in the absence of external torque). The presented measurements show the evolution of the Toroidal plasma rotation over the sawtooth period by conditionally resampling measurements from a large number of resolved sawteeth events. In contrast to the previous measurements that show the plasma rotation averaged over several sawteeth, this measurement resolves the Toroidal rotation changes across a canonical sawtooth. Initial results indicate a fast ($< 2ms$) co-current acceleration at the sawtooth crash in the plasma core followed by a profile relaxation on a time scale $\sim$5ms until the next sawtooth event. Outside the sawtooth inversion radius there is a smaller counter-current acceleration, implying some momentum conservation, with an total co-current acceleration contribution in agreement with previous measurements.

1. Introduction

Understanding the behaviour of tokamak plasma rotation and momentum transport in general, is the subject of intense present day experimental and theoretical research [1, 2, 3, 4, 5, 6, 7]. Plasma rotation and velocity shear are known to play an important role in the formation of transport barriers such as H-mode and ITBs and Toroidal rotation may help stabilise resistive wall mode (RWM) instabilities[8]. Furthermore, bulk plasma rotation has been observed to change synchronously with other changes in plasma behaviour, modify the plasma electric field and ExB shear that are though to reduce turbulence, increase the threshold for NTM modes etc [9, 10]. Recent interest in the mechanisms that can drive intrinsic plasma rotation (i.e. in the absence of an explicit external torque such as a neutral beam) has been heightened with the conclusion that in fusion devices such as ITER, external torques will not determine the overall plasma velocity stimulating a quest for an improved understanding of the physical mechanisms involved [11]. In view of the lack of a theoretical model, empirical scalings for Toroidal rotation scaling have been constructed using data from many machines that predict a considerable rotation in larger machines [12]. The need for more information and a viable model is still urgent.

Following the installation of a diagnostic neutral beam on the TCV tokamak [13], together with a spectroscopic diagnostic system (described below), intrinsic rotation has been reported over a wide variety of plasma conditions [14, 15, 16, 13]. In the initial experiments on a simple limited discharge, the maximum Toroidal rotation was found to scale inversely with the plasma current and approximately proportionately to the ion temperature (It is to be recalled that since TCV does not yet feature direct ion heating, ion heating is determined by electron-ion collisions). The Toroidal rotation profile gradient was similar to the ion temperature gradient in line with other experimental observations and theoretical investigations that suggested a strong coupling of the ion heat and momentum transport [14, 17]. There is an ever increasing number of reported Toroidal rotation behaviour in the literature indicating that, contrary to initial expectations, plasma rotation is affected by many kinds of heating and plasma instabilities present in today's and most probably tomorrow's devices.

This paper continues with an instigation of a relatively simple limited discharge configuration. Fig. 1 shows the Toroidal rotation profiles for a series of similar discharges on TCV in which the plasma current

---

*See list in S. Coda et al., paper OV/5-2, this conference

was varied. The rotation gradients outside the sawtooth inversion radius (STIR) are similar with a co-current profile flattening appearing inside the STIR. Using ECH heating outside the sawteeth inversion radius Fig. 2, that displaces the STIR inwards, the rotation gradient was maintained up to the displaced STIR resulting in increased core rotation.
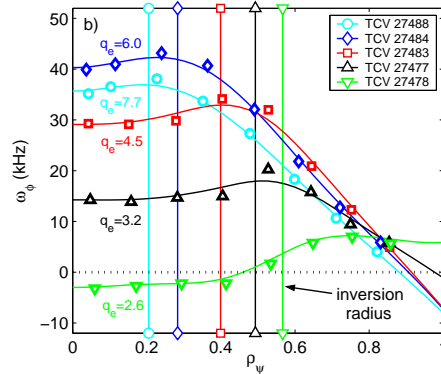
FIG. 1. Toroidal rotation profiles for a sequence of limited discharges with a range of plasma currents. Rotation always in the counter-current direction, the velocity gradient in the plasma edge is discontinuous at the sawteeth inversion radii indicated by vertical lines
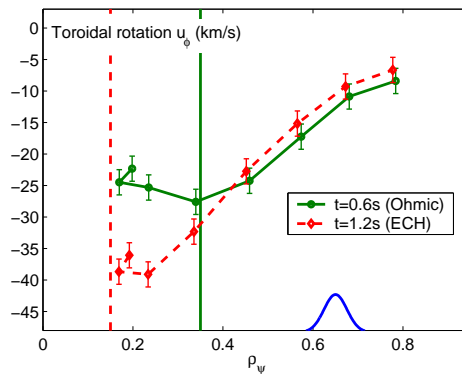
FIG. 2. Toroidal rotation profiles for two discharges with and without ECH heating outside the sawtooth inversion radius (position $\rho_\psi \approx 0.6$ indicated) that has the effect of displacing the inversion radius towards the plasma core. In both cases, the Toroidal rotation profile in the edge extends up to the sawtooth inversion radius

By combining these observations, the core rotation, extrapolated from the edge slope, was found to be relatively constant for high q (low current) discharges until q reaches values ~ 3 and below which the whole rotation profile changes significantly[16]. These plasmas are ohmically heated and the ion temperature depends on the electron temperature that in turn depends on the electron temperature. Using the ion temperature scaling described above, the constancy of the extrapolated core rotation in the absence of sawteeth is further improved Fig. 3 [18]

These observations correspond to a discharge with regular sawteeth for which an average co-current torque appears to act on the plasma core inside the sawtooth inversion radius. The measurements are made across several sawteeth so only the average torque in measured. In order to gain some insight into the torque generation physics, it is necessary to look at the rotation evolution during a sawtooth cycle. In widely accepted sawtooth reconnection model, at the sawtooth crash, there is a strong particle and energy mixing often accompanied by an expulsion of a heat and particle pulse outwards from the plasma core. This paper reports an initial investigation of the momentum generation and transport time resolved within a sawtooth cycle.
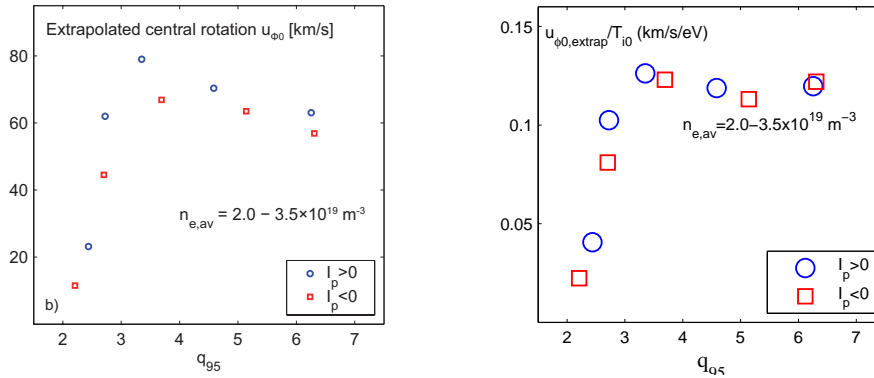
FIG. 3. Left: Extrapolation of the axial Toroidal velocity from the gradient outside the sawtooth inversion radius. Right: Same data normalised to the ion temperature. Without sawteeth, this implies that the plasma current scaling reported previously [14] can be explained by an effect of the sawteeth presence

2. Experimental Procedure

On the diagnostic front, several plasma devices across the world are equipped with systems that are able to provide plasma rotation profiles time resolved across the plasma discharge so that the evolution of the plasma rotation profiles may be measured on a regular basis across wide range of plasma parameters and operational scenarios. As many of these systems employ Charge Exchange Recombination Spectroscopy (CXRS or CHERS) using the light emitted from the interaction of a high power Neutral Heating Beam (NBI) with the plasma, the measured rotation profiles are often dominated by the applied torque and not the intrinsic plasma physics. To measure the intrinsic rotation, short, and hopefully non-perturbing, NBI pulses are sometimes used or passive spectroscopy of impurity atoms radiating in the plasma core [2].

On the TCV tokamak, a low power Diagnostic Neutral Beam (DNBI) is used whose torque on the plasma may be neglected but whose beam energy is sufficient to penetrate across the whole plasma radius. It provides time resolved ion density, temperature and rotation profiles time resolved across the discharge period [13]. TCV features an almost complete Carbon tile wall protection and Boronisation conditioning such that Carbon is the strongest intrinsic plasma impurity so the $CVI(n = 8 \rightarrow 7)$ is used for most measurements. TCV also features a comprehensive shaping and control system without a fixed divertor chamber so that a wide variety of plasma shapes and configurations may be examined between and possibly during the $\sim 2s$ plasma pulse [20]. A high power X2 (second harmonic) ECH heating system with launchers that may be controlled during the discharge permits precision ECH and ECCD (current drive) during the plasma discharge and a high power X3 (third harmonic) heating system is available to heat higher density plasmas.

Since the sawtooth period for these discharges is often a few ms and the standard CXRS system uses integration periods in excess of 20ms for 20 radial chords, several modifications were introduced to obtain time resolved velocity measurements. It is well documented that by depositing co-current ECCD just outside the STIR together with power deposition in the plasma core, the sawteeth are partially stabilised with the sawtooth period rising from a few to over 15ms [**?**]. For these experiments, the main Toroidal field (B_ϕ) was reduced from the normal 1.43T to $\sim$1.2T with the EC beam launched from the equatorial plan displacing the resonance to the inboard side of the plasma. At a plasma current $I_p = -260$ kA, with $n_{e,av} \approx 1.5 \times 10^{19}\,\mathrm{m}^{-3}$, $q_e = 2.7$ was obtained, with a $q = 1$ surface located at $\rho_\psi \approx 0.6$. The power and deposition profiles were initially calculated with the TORAY-GA code and the radial location of the current drive tuned by fine scans of B_ϕ whilst keeping the ration B_ϕ/I_p, and thus q_e, constant or by small scans of the ECCD injection angle.

When reducing the detector integration time from $\sim 30ms$ to $\sim 2ms$ two problems arise. The number of sampled chords has to be reduced due to detector readout constraints and the acquired light intensity is insufficient to obtain sufficient signal over a single sawtooth event. The number of observation chords

was reduced from 20 to 4, but this reduction in the spatial resolution was partially mitigated by integrating adjacent chords and choosing effective observation chords distributed approximately equally across the plasma minor radius. Thus, although only 4 chords are now available, they may still be chosen to monitor the core and peripheral rotation evolution.
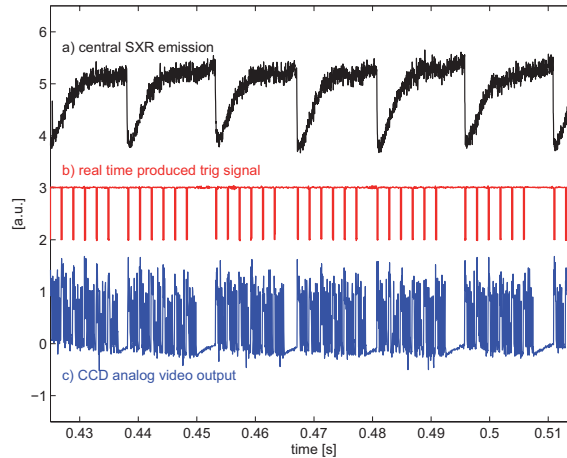
FIG. 4. Traces showing the triggers provided to the CXRS detector system by the Real Time system. The soft X-ray emission intensity in the upper trace shows the sawteeth evolution, the middle trace the triggers sent to the CXRS detector and the lower trace the detector video output

To compensate for the reduction in signal caused by the reduced integration time, a conditional sampling technique was developed in which the signal from several sawteeth crashes was summed as a function of the sawtooth phase. Conditional resampling requires that the acquisition time uncertainty, within the phase of the sawtooth, be considerably less than the target 2*ms* time resolution. This was achieved by implementing a real-time (RT) trigger system based on a digital control system recently installed on TCV [20]. The sawtooth evolution, detected by plasma spectral emission using a soft X-ray detector, is monitored by the RT system and a sequence of regularly spaced triggers is sent to the CXRS detection system upon sawtooth detection. The CXRS CCD cameras effectively integrate the incident signal until receiving a trigger that causes the signal to be electronically read-out and stored. This means that the first trigger from the RT system, programmed to occur during the initial sawtooth crash, is almost entirely a measurement of the plasma rotation just *Before* the sawtooth crash and the subsequent triggers measure the average plasma rotation during successive 2*ms* integration periods, Fig. 4 and Fig. 5.
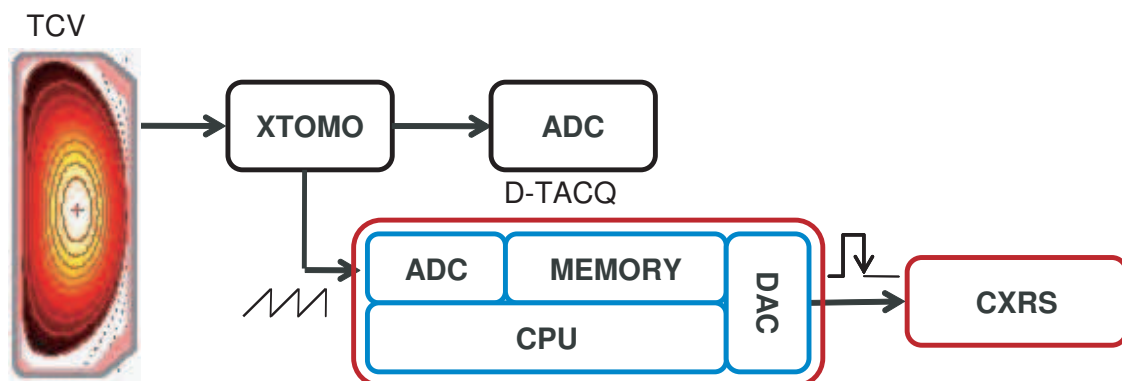
FIG. 5. Schematic of the TCV Real Time Control System used to trigger the CXRS system. The soft X-ray signal is acquired as usual and by the Real Time node where a software algorithm detects the sawtooth event. The Real Time node then generates TTL triggers from its DAC that are sent to the CXRS detector

For these experiments, the DNB injector operated with a regular 15ms on 15ms off duty cycle that was not synchronised to the sawteeth events. The TCV CXRS diagnostic subtracts the spectra before neutral

beam injection from that with the beam to obtain the *active* spectrum i.e. that due to the beam interaction with the plasma. In this fast acquisition configuration, following a completed acquisition, the acquired spectra were divided into those encompassing sawteeth events with and without the presence of the DNB current. Each 2*ms* acquisition period was then sorted with respect to its time from the preceding sawtooth crash. By averaging the spectra in each category and extracting the *active* spectra by subtraction, the evolution of an *average* or more correctly *canonical* sawtooth was constructed.

3. Results and Discussion

Partially stabilised sawteeth resulting from judicious ECCD and/or ECH tend to have a relatively strong soft X-ray sawtooth signature. The quality of the real-time triggering system is demonstrated in Fig. 6. The soft X-ray signal is divided by the detected crash time and the signal is shown over-plotted across the experimental period together with an average trace. In spite of the varying sawtooth period, demonstrated by the start of the next sawtooth crash visible on the RHS of the plot, the sawteeth are remarkably similar, providing credibility to the conditional resampling method. The average sawtooth appears to have a second partial crash after $\approx 5ms$ but the initial sawtooth crash should be well diagnosed with the available 2*ms* time resolution. A statistical analysis of the summed spectra indicated an uncertainty of order ± 1 km/s that is of the same order of the uncertainties inherent to the CXRS measurement (e.g. wavelength calibration) [19].
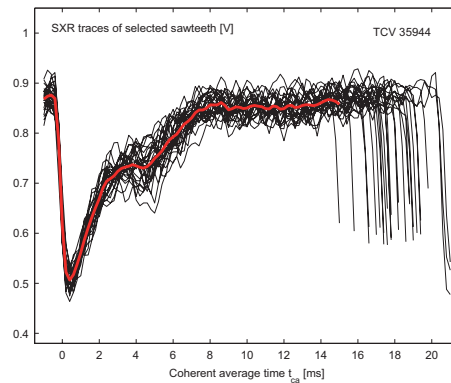
FIG. 6. SXR traces for sawteeth selected for the coherent average analysis. The average trace, superimposed in red shows some indication of a partial reconnection at $t_{ca} = 5$ ms (TCV 35944).

The temporal and spatial evolution for a canonical sawtooth in one discharge is shown in Fig. 7. In the upper plot, the Toroidal rotation profile is shown: just after the crash, near the middle of the sawtooth period and near the end of the sawtooth period. A clear co-current "kick" in the core is seen at the sawtooth crash but the profile then rapidly relaxes to one that evolves more slowly until the next crash. The Toroidal velocity at three radial locations is shown as a function of time relative to the sawtooth crash in the lower plot. It is important to recall that the acquired spectra are the average over a relatively wide radial region (from the signal integration on the CXRS detectors), and that each point results from the integrated signal ± 1ms. Again, the strong co-current "kick" in the plasma core is well presented and the Toroidal rotation evolves little across the sawtooth period at the STIR ($\rho_\psi \approx 0.4$). The rotation well outside the STIR reacts slowly to the core change and recovers its pre-sawtooth value on about the same time scale as the core rotation, if the initial change is excluded. The main result here is that the strongest core rotation change occurs well below the 2*ms* time resolution of this experiment and there then appears to be a smooth momentum redistribution before the next sawtooth. From the previous measurements, it is already known that the overall effect is to generate an effective co-current torque in the plasma core but this result also demonstrates some degree of momentum conservation across the plasma profile with the plasma outside the STIR accelerating in the opposite direction to the core, albeit on a considerably longer timescale.

The reproducibility of this experimentally challenging result is shown in Fig. 8 where the profile change across the sawtooth for several discharges with the same STIR are plotted. This is simply the difference between the first rotation profile following the sawtooth crash and the best estimation of the profile just
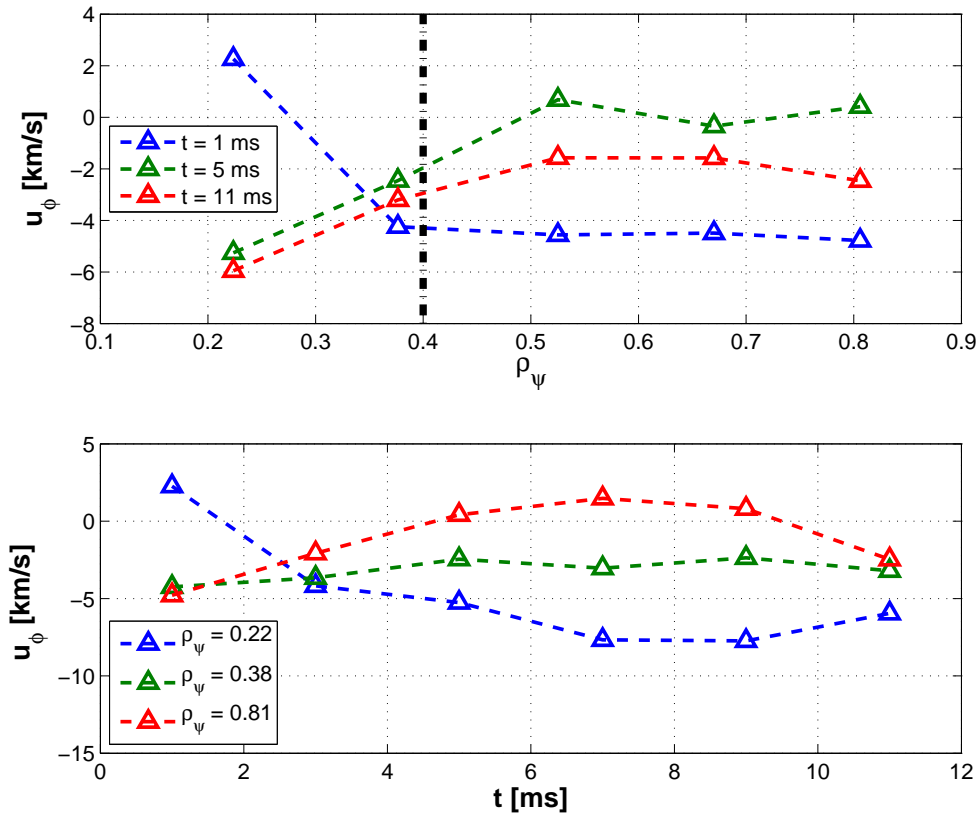
FIG. 7. *Upper figure shows the Toroidal rotation profile at 1, 5 and 11ms after the sawtooth crash. There is a clear co-current "kick" in the plasma core at the sawtooth crash. Lower figure shows the evolution of the Toroidal rotation at three radial positions across the complete sawtooth period. The fast acceleration at the sawtooth crash is followed by a slower velocity profile evolution before the subsequent sawtooth*

before the crash. Again, the profile appears to pivot around the STIR with the core showing a strong Co-Current acceleration whereas the rest of the plasma is slightly accelerated in the counter-current direction. One set of *typical* error bars are shown to indicate the calculated measurement uncertainty.

The evolution of T_e in TCV plasmas in the presence sawtooth activity and with ECH power, has been modeled using the ideas in the theoretical model from Porcelli [22]. The sawtooth crash is modeled using the Kadomtsev [23] theory of full or partial reconnection, in which topological constraints combined with particle and thermal energy conservation, are invoked to determine the relaxed post-crash T_e profile, as a function of the pre-crash profile.

With the conjecture that this may be applicable to momentum transport too, the spirit of this model can be extended to include Toroidal momentum and velocity where the mixing rules for Toroidal rotation profiles are derived by observing the formal correspondence between thermal energy $p_e = n_e T_e$ and Toroidal momentum $p_\phi = m_i n_i u_\phi$ [24]. For the sawteeth, it was found that, depending on the degree of peaking of the pre crash T_e profile, the post-crash radial profile may be hollow (*hot ring*), flat or slightly peaked.

An initial estimation of this effect on plasma rotation in TCV Ohmic discharges was implemented in the ASTRA transport code by including the mixing rules for Toroidal rotation profile. A simplified parabolic rotation profile was introduced with a peaking exponent α i.e. $(1 - r^2/a^2)^\alpha$, and the transport tuned to match the velocity profile relaxation time to the observed $\sim 5ms$. A hollow rotation profile, in qualitative agreement with the TCV results, was obtained especially for peaking factors α greater than unity [19]. In
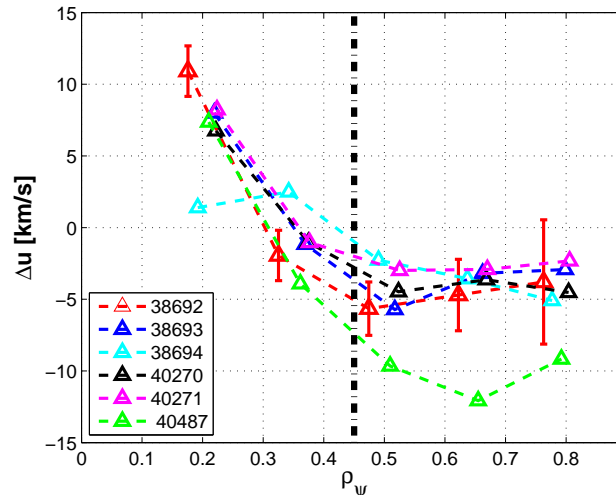
FIG. 8. *The change in the rotation profile just before and just after the sawtooth crash for several discharges. There is a strong co-current plasma acceleration in the core and a smaller counter-current acceleration outside the sawtooth inversion radius.*

spite of the assumptions, it is, at least, not inconsistent to model the Toroidal rotation behaviour together with the density and electron temperature behaviour. The resulting net plasma torque may not, however, be described by momentum distribution alone. A heuristic model for the acceleration that is always in the co-current direction has been attempted where a strong electric field develops during the magnetic reconnection (sawtooth) from a variation in the poloidal magnetic flux [19]. Initial estimates give a core electric field of the order of a few V/m that could be sufficient to drive the observed velocity change. In this model, the ions were supposed to accelerate freely over the sawtooth crash time but a more plausible model would require a model for the ion viscosity and friction forces on these time scales and consider the difference in the effect of such an electric field on the main and impurity ions. More detailed rotation profile measurements would be extremely useful in indicating whether this kind of understanding could be pertinent.

The reduced spatial resolution means that only one spatial chord monitors the plasma core. Although increasing the temporal resolution is possible, the limited beam/plasma luminosity of the CXRS system will limit the possibilities. New detectors with faster readout but the same over 80% quantum efficiency are being installed on the TCV CXRS that should result in up to 40 observation chords across the plasma minor radius. Following the initial observations, there remained a certain amount of doubt in the possible interpretation since only the central observation chord, for the profile immediately following the sawtooth crash, shows a strong discontinuity. Since then, all the diagnosed discharges have shown a similar effect that can no longer be ascribed to an instrumental uncertainty but, here again, a more detailed profile would be helpful.

4. Conclusions and Outlook

This paper presents the first time resolved measurement of Toroidal plasma rotation profiles across saw-teeth events. Although the experimental technique is quite involved, the measurement shows that a strong co-current acceleration occurs in the plasma core on a time scale that appears considerably faster than the 2*ms* time resolution used here can resolve. In essence, the rotation profile is found to be directly affected by the *sawteething* phenomenon. A degree of momentum conservation close to the crash is observed with the rest of the plasma accelerating in the opposite (counter-current) direction but the overall effect is to exert a cumulative torque on the plasma core that, as previously reported, limits the core velocity. The momentum pinch demonstrated by the constant velocity gradient in the plasma edge, if uninterrupted by the sawtooth mixing, would appear to result in a peaked rotation profile, at least for these discharges. The initial scaling law for the maximum Toroidal rotation velocity thus appears to be caused by the sawteeth rather than some effect of the plasma current on the momentum transport physics.

Measurements with higher spatial resolution, and possibly higher temporal resolution, are being planned in the near future to see if there is further spatial or temporal structure in this process that may help test a model for momentum redistribution and torque generation by sawteeth and possibly other strong mode activity.

Acknowledgements

References

[1] J.S. deGrassie, Plasma Phys. Control. Fusion **51** 07413335 (2009)
[2] J.E. Rice, *et al* Plasma Phys. Control. Fusion **50** 124042 (2008)
[3] W.M. Solomon, *et al*, Nucl. Fusion **49**, 085005 (2009)
[4] P.C. de Vries, *et al*, Nucl. Fusion **48**, 065006 (2008)
[5] P.H. Diamond, *et al*, Nucl. Fusion **49**, 045002 (2009)
[6] A.G. Peeters, *et al*, Physics of Plasmas, **16**, 042310 (2009)
[7] Y. Camenen, *et al*, Physics of Plasmas, **16**, 012503 (2009)
[8] H. Reimerdes, *et al*, Physics of Plasmas, **13**, 056107 (2006)
[9] K.H. Burrell, Physics of Plasmas, **6**, 4418 (1997)
[10] H. Reimerdes, *et al*, Phys. Rev. Lett. **98**, 055001 (2007)
[11] E.J. Doyle, *et al*, Nucl. Fusion **47**, S18 (2007)
[12] J.E. Rice, *et al*, Nucl. Fusion **47**, 1618 (2007)
[13] B.P. Duval, *et al*, Physics of Plasmas, **15**, 056113 (2008)
[14] A. Scarabosio, *et al* Plasma Phys. Control. Fusion **48** 663 (2006)
[15] A. Bortolon, *et al*, Phys. Rev. Lett. **97**, 235003 (2006)
[16] B.P. Duval, *et al* Plasma Phys. Control. Fusion **49** B195 (2007)
[17] J.S. deGrassie, *et al*, Nucl. Fusion **43**, 142 (2003)
[18] B.P. Duval, *et al*, Proceedings of the 35rd EPS,Hersonissos **P-2.020**, Greece (2008)
[19] A. Bortolon, PhD Thesis No 4569, EPFL-Lausanne (2009), http://library.epfl.ch/theses/?nr=4569
[20] J.I. Paley, *et al* Plasma Phys. Control. Fusion **51** 124041 (2009)
[21] C. Angioni *et al*, Nucl. Fus. **43** 455 (2003)
[22] F. Porcelli, *et al*, Plasma Phys. Control. Fusion **38**, 2163 (1996)
[23] B.B. Kadomtsev, Sov. J. Plasma Physics **1**, (1976)
[24] I. Furno, *et al*, Nucl. Fusion **41**, 403 (2001)